JOURNAL OF MATERIALS SCIENCE 19 (1984) 2073–2078

The effect of pore size and heat treatment on the fracture toughness of pressed and sintered Ancoloy SA powdered steel

J. T. BARNBY
Department of Metallurgy and Materials Engineering, University of Aston, Birmingham, UK
D. C. GHOSH
Al-Fateh University, Libya

Ancoloy SA powder, adjusted by addition of carbon to give a composition which was slightly hypo-eutectoid, was tested in a pressed and sintered condition. Porosity was varied by changing the pressing pressure and structure was varied by heat treatment. The effect of pressing pressure, through void content and shape, dominated the toughness change, although heat treatment produced a large increase in yield stress.

1. Introduction

Fabrication using powder methods can provide economic and low energy routes for the production of metal components. There is no reason to aim for identical properties to those of forged and machined components so long as the powder products have adequate properties to meet service conditions. In order to ensure that this is so, accurate values of critical properties must be known. These critical properties are likely to be mechanical strength, fracture toughness and fatigue resistance.

Previous work [1] has shown that the fracture toughness (K_{IC}) of a range of sintered steels rose linearly with yield stress up to yield stresses of around $500\,MN\,m^{-2}$. Ingelstrom and Ustimenko [2] have made similar observations on a series of pressed and sintered steels and on sinter-forged steels. These authors emphasize the importance of porosity on mechanical properties as do Billington and Torabi [3] and Billington *et al.* [4] in relation to the properties of hot consolidated steel strip.

The work below is part of a wider programme which seeks to define more clearly the role played by the pores remaining after a pressing and sintering operation. Once this rule is well understood the way will be cleared for further developments in sintered steels.

2. Experimental methods and materials

2.1. Materials

The Hoganas Ancoloy SA powder is a pre-alloyed powder made from sponge iron to which finely divided alloying elements are diffusion bonded. This powder was mixed in a rotary drum for 25 minutes with 0.6% graphite and 0.65% zinc stearate by weight. The powders were compacted into rectangular specimen blanks in a closed die at pressures of $3978\,MN\,m^{-2}$ or $598\,MN\,m^{-2}$ to produce densities of 6.7 or $6.9\,Mg\,m^{-3}$, respectively.

Sintering was carried out at 1120° C for one hour in an atmosphere of 90% nitrogen and 10% hydrogen. The blanks were cooled in this atmosphere after withdrawal from the hot zone of the furnace. Machining and notching were carried out on such blanks. One batch of specimens was tested in this condition. A further set was austenitized at 850° C for 30 minutes, oil quenched and tempered at 175° C for one hour in air. These latter specimens had their surfaces reground to clean them. Samples of each type were analysed after heat treatment. Their constitutions are shown in Table I. The final densities of the sintered (ASA-S) or sintered quenched and tempered (ASQ-SQT) materials were $6.7\,mg\,m^{-3}$ and $6.9\,Mg\,m^{-3}$, depending on pressing pressure. These materials had yield stresses as shown in Table II.

0022–2461/84 $03.00 + .12

TABLE I Chemical constitution of alloys (wt%)

	Sintered	Sintered, quenched and tempered
Cu	1.42	1.43
Ni	1.64	1.66
Mo	0.55	0.56
C	0.65	0.79
Si	0.20	0.20
Fe	Balance	Balance

2.2. Toughness test

Fracture toughness tests were carried out in triplicate to conform to the BSI standard number 5447 [5] using a three-point bend specimen with a gross width of 25 mm, a thickness of 12.5 mm, and an overall length of 110 mm. In addition similar tests were performed on specimens with controlled root radii at the notch tips rather than with fatigue-cracked notches.

2.3. Metallography and pore size measurement

Metallographic specimens were impregnated with an epoxy resin under vacuum. The resin was cured before grinding and polishing the specimens.

Fracture surfaces were examined in a scanning electron microscope by cutting a section from the fracture surface about 2 to 3 mm thick.

Pore areas and distributions were determined using a Quantimet 720 optical microscope system. After normal grinding and diamond polishing the surfaces were etched with 5% nital to remove metal which might have flowed into the pores. Fine polishing then removed the rounded pore edges. The areas occcupied by pores of various sizes were then estimated by counts of 250 fields each of 0.0115 mm^2 at an optical magnification of x315 enlarged to x1300 by projection. Thus the counts correspond to a survey of 2.87 mm^2 of surface in each case, the 250 fields being random.

3. Results

3.1. Fracture toughness

Standard fracture toughness tests, carried out in triplicate, using pre-fatigue cracked notches, gave K_{IC} values as listed in Table II.

3.2. Metallography

Microstructures of the ASA-S showed ferrite and cementite, Fig. 1a, and the ASA-SQT material showed a tempered martensite as shown in Fig. 1b. Fractography showed that all fracture surfaces were of the ductile dimple type with at least two clear families of dimple sizes (Fig. 1c), the smallest being around 2 to 3 μm in diameter.

3.3. Pore distribution

The pore distribution shown in Fig. 2 was obtained by feature analysis, where the area of each "pore" was considered individually, and the number falling into each size category was recorded. The area parameter for each phase was chosen, since the voids were of irregular shapes of random orientation, and the particular diameter would not have given as true a measure of size distribution.

Attempts to measure the inclusion contents of the specimens failed due to the fact that the inclusions were predominantly fine oxides, and had a similar reflectivity to the "pores". As a result, separate detection "thresholds" for pores and inclusions could not be operated, and therefore only one result was recorded combining the voids and inclusions and termed "pores". Treating the inclusions as "pores" also simplifies the analysis, as the matrix–particle interfacial strength is not significantly high.

As shown in Fig. 2, large numbers of "pores" are in the size range of 3 to 8 μm^2. The nearest approximation would be to consider that the majority of inclusions are in this range, and that the majority of voids are in the size range of 100 to 200 μm^2. The existence of the wide range of sizes and shapes of voids is also supported by the

TABLE II Fracture toughness values and mean yield stresses of steels from triplicate tests

Alloy	Density ($Mg\,m^{-3}$)	Yield stress ($MN\,m^{-2}$)	Volume fraction voids (%)	K_{IC} ($MN\,m^{-3/2}$)	Elongation (%)
ASA-S	6.7	427	15.5	24.9	2.5
ASA-S	6.9	471	12.2	28.5	3.0
ASA-SQT	6.7	658	15.5	25.8	1.5
ASA-SQT	6.9	733	12.2	29.6	1.5

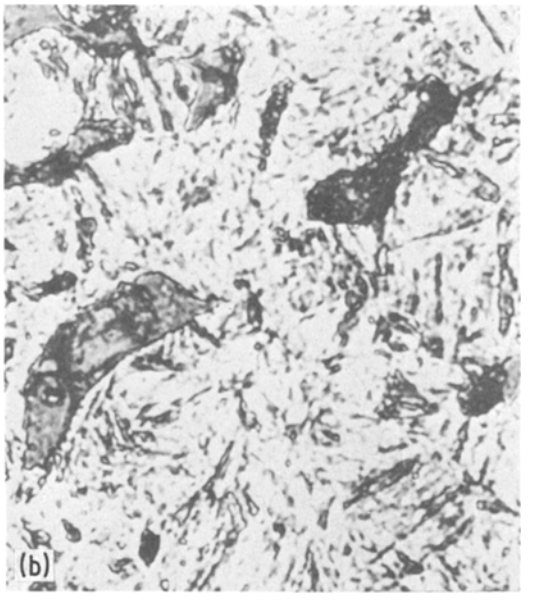

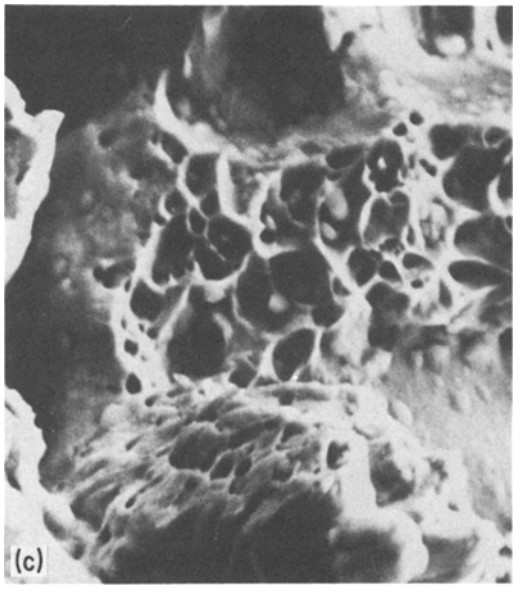

Figure 1 Microstructure of the sintered steels. (a) Typical microstructure of Ancoloy SA compact. Sintered, ×1150. (b) Microstructure of Ancoloy SA compact. Sintered, quenched and tempered, ×1150. (c) Ductile dimples in Ancoloy SA compact, ×1790.

use of scanning electron microscope. It is believed that the figures show real distributions although inclusions in the size range of 2 to 3 μm across are not distinguishable from voids to the counting instrument used. The examples of voids in the two types of materials studied are shown in the scanning electron micrographs of Fig. 3. From such photographs, at higher magnifications, it was possible to measure the minimum radii of curvature for the pores, which are generally complex in shape. These radii were near to 0.1 μm in most cases.

3.4. Tests on blunt notched specimens

Tests similar to fracture toughness tests were carried out using notches with controlled tip radii rather than with fatigue cracked roots. Four sets of ASA compacted specimens (3 in each set) in two levels of densities were machined and notched to a depth of 0.45 W with root radii of 0.127, 0.254, 0.508 and 0.762 mm. One set of two specimens of the above compact specimens, for both levels of densities, were initially machined and notched to a depth of 0.3 W, with root radius of 0.127 mm, and fatigue cracked to a depth of 0.45 W. This helped to produce infinitely small root radius (~ 0) at the crack tip. The tip radii of notches of other specimens were measured, before testing, by optical examination in a microscope. Fig. 4 shows the variation of apparent toughness of such specimens as function of the notch tip radius.

4. Discussion

Table II shows an almost identical increase in toughness with decrease in porosity for both materials, even though the quenched and tempered material had a yield stress much enhanced by the

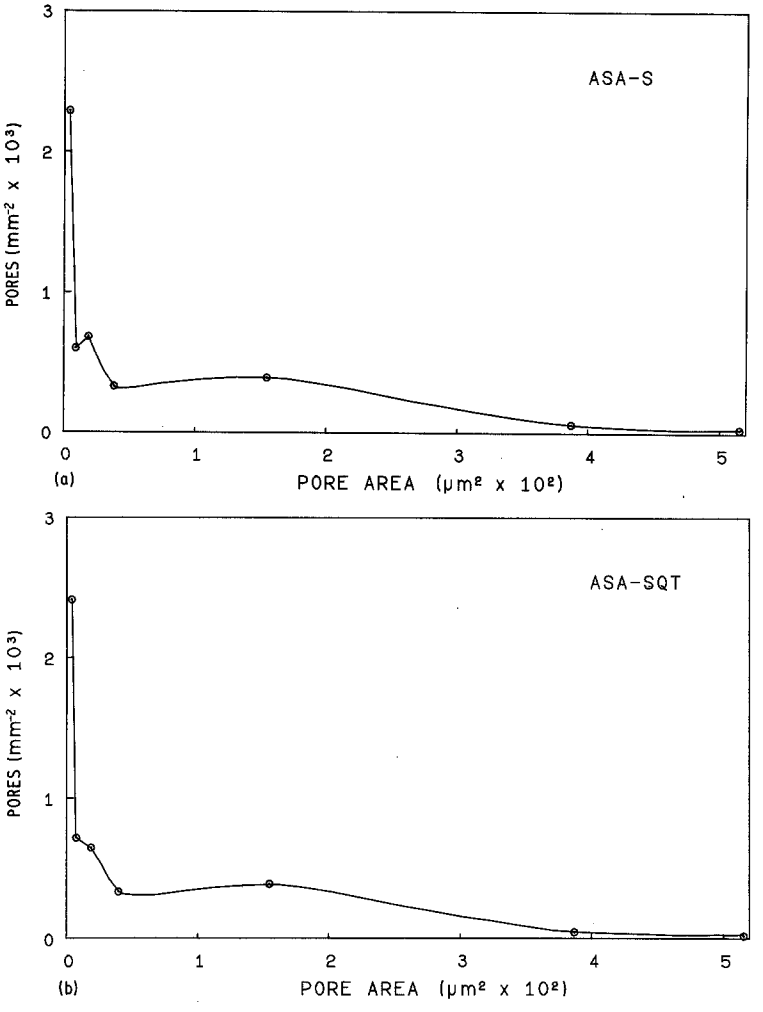

Figure 2 Pore size distributions for the sintered steels. (a) Ancoloy SA, sintered material (ASA-S). (b) Ancoloy SA, sintered, quenched and tempered (ASA-SQT).

heat treatment. It therefore appears that porosity controls the fracture resistance of the material, though increases in yield stress by heat treatment are accompanied by small increases in toughness.

The fractography results clearly show that the micromechanism of fracture is the englargement and coalescence of voids. Theories of this process are not well advanced [6, 7] and as yet there is no

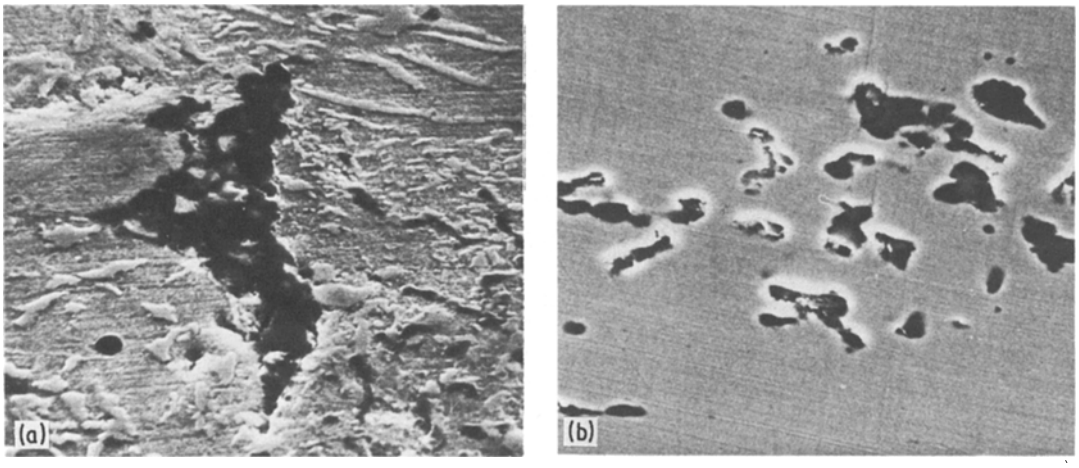

Figure 3 Scanning electron micrographs showing pores. (a) ASA-S material, ×5800. (b) ASA-SQT material, ×3200.

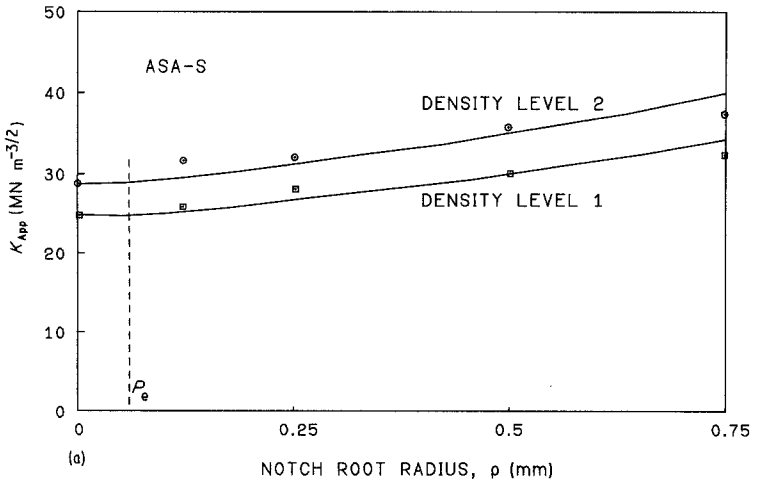

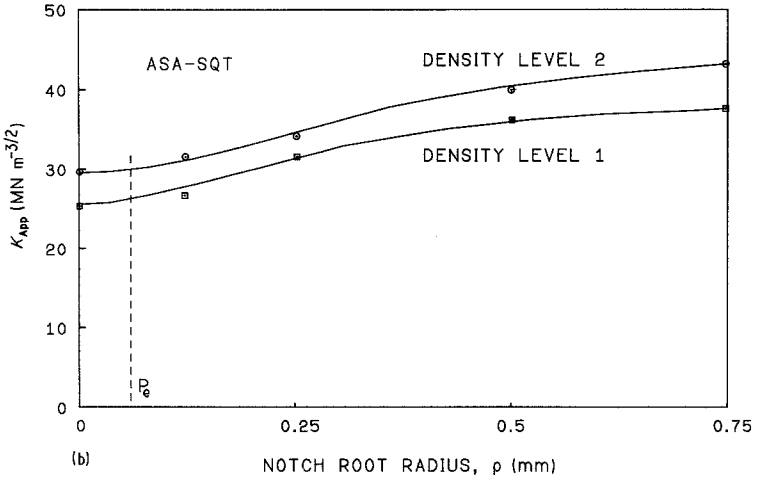

Figure 4 Variation of the apparent toughness of the sintered steels with notch root radius. The value placed at zero radius is the toughness for fatigue cracked notches. (a) ASA-S material, (b) ASA-SQT material.

successful treatment which is capable of predicting toughness from the distribution of voids in a matrix of known properties. This may arise partly because practical structures are far from the idealizations of models of uniform spherical or cylindrical holes. The pore distributions indicate high numbers of very small voids, in contrast with the results of other workers [2]. In both sets of experiments small inclusions would be counted as voids so the difference probably arises from differences in the starting powders and processing techniques.

Though in these alloys there were large numbers of very small voids it is far from clear that these small voids are of dominant importance: in fact rather the opposite. Examination of the larger voids showed that they contained surface features with local radii of curvature of about 0.1 μm. These constitute larger stress concentrators than the small voids. Also, the effective length of the larger voids is not accurately known since they are in fact interconnected [8].

The fracture toughness values, K_{IC}, allow an estimate of the crack tip radius at the point of fracture if we assume the radius to be $\delta_c/2$ where δ_c is the critical crack opening displacement [9]. Using the equation

$$\sigma_{ys}\delta_c = K_{IC}^2(1-\nu)/E$$

where σ_{ys} is the yield stress, we may estimate δ_c providing that Poisson's ratio, ν, (which we assume to be 1/3), and Young's Modulus, E, are known. The Young's modulus is dependent on porosity through the relation [10]:

$$E = (1-\epsilon)^{3.4} \times 206\,\mathrm{GN\,m^{-2}}$$

The actual volume fractions of pores, ϵ, are given in Table II for the materials tested here. Using these values we find $\delta_c/2$ to be about 2 to 3 μm for these steels. This figure is much greater than the sharpest stress and strain concentrator present in the structure, which as we have seen, has a radius of about 0.1 μm. Thus during crack propagation these sharp radii must concentrate local

strains, and in doing so blunt themselves out by a factor of 20 to 30 times.

In agreement with earlier findings on lower strength sintered steels [1] we find that for the materials tested here fracture toughness tests on specimens with notch tip radii of 0.1 mm are very similar to results from properly fatigue-cracked specimens. This probably arises because pores effectively sharpen the notch tip so long as the final machining operation on the notch is a delicate one which does not produce a heavily deformed region below the cutting tool. This is so when radii as fine as 0.1 mm are cut.

The dimple fractures show voids of various sizes down to diameters of 1 and 2 μm. These small dimples or voids are often clearly associated with inclusions. Thus the information is consistent with a view that the process of fracture commences when acuities of 0.1 μm radius, on the sides of voids of around 10 μm diameter, concentrate the plastic strain until a local displacement of δ_c, that is between 4 and 6 μm, blunts the radius to $\delta_c/2$. At such a stage local damage to particles such as carbides or inclusions opens up a void sheet which interconnects large voids. The process then repeats itself. Such a process is idealized in Fig. 5. Clearly the void sheet could form and open up equally well under the action of pure shear displacements also localized by sharp stress concentrations. It also seems likely that stages (b) and (c) in Fig. 5 are the mechanisms by which general yield spreads across the section of a tensile specimen, and therefore constitute the yield mechanisms. We would therefore expect the observed linear increase in toughness with yield stress for a given metallographic structure, and a broad relation of this type for roughly similar structures.

5. Conclusions

Toughness, or resistance to crack propagation, is mainly controlled by porosity in the materials investigated. The percentage increase in yield stress arising from heat treatment is not parallelled by a similar increase in fracture resistance. Larger gains in fracture resistance would accrue from elimination of pores or changes in the morphology of pores.

The implications for design are that heat treatment can be used to allow higher working stresses so long as stress concentrators such as notches are absent. The advantages in strength developed by heat treatment will be progressively lost as stress concentrations mount in the design.

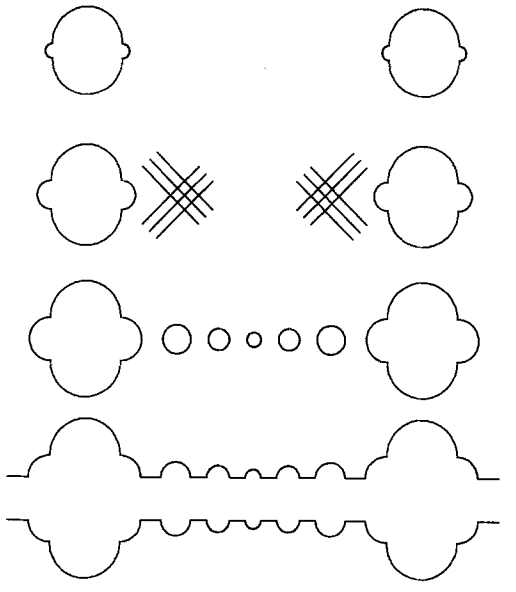

Figure 5 Idealization of the process of local yield and ductile fracture commencing from voids in sintered steels.

There are also implications of the present work to failure by fatigue. Fatigue properties of the materials investigated here have been examined by the authors and are the subject of a further paper.

References

1. J. T. BARNBY, D. C. GHOSH and K. DINSDALE, *Powder Met.* **16** (1973) 55.
2. N. INGLESTROM and V. USTIMENKO, *ibid.* **18** (1975) 303.
3. J. C. BILLINGTON and A. TORABI, *ibid.* **20** (1977) 162.
4. J. C. BILLINGTON, D. E. FALLAS and A. TORABI, *ibid.* **18** (1975) 323.
5. British Standard No. 5447 (1977).
6. D. M. TRACY, *Eng. Fract. Mech.* **3** (1971) 301.
7. J. R. RICE and D. M. TRACY, *J. Mech. Phys. Solids* **17** (1979) 201.
8. M. WARD, PhD Thesis, University of Aston in Birmingham (1977).
9. R. W. NICHOLS *et al.*, "Practical Fracture Mechanics for Structural Steel", edited by M. O. Dobson (Chapman and Hall, London, 1969).
10. G. D. McADAM, *J. Iron Steel Ints.* **168** (1951) 347.

Received 8 September
and accepted 22 September 1983